J. Fluid Mech. (1977), *vol.* 79, *part* 4, *pp.* 669–688
Printed in Great Britain

The unsteady laminar boundary layer on a rotating disk in a counter-rotating fluid

By R. J. BODONYI

Department of Mathematical Sciences, Indiana–Purdue University of Indianapolis, 1201 East 38th Street, Indianapolis, Indiana 46205

AND K. STEWARTSON

Aerospace Engineering Department, University of Southern California, Los Angeles†

(Received 22 January 1976)

The growth of the unsteady boundary layer on an infinite rotating disk in a counter-rotating fluid is examined numerically and analytically. The numerical computations indicate that the boundary layer breaks down when $\Omega t^* \approx 2{\cdot}36$ in a novel way: the displacement thickness, as well as all the velocity components, becomes infinite. This numerical solution is fitted to an asymptotic expansion which contains the singularities found in the numerical integrations, and it is concluded that the solution of the unsteady similarity equations does break down at a finite time as the numerical results indicate. This problem is placed in a physically more realistic context by considering numerically the unsteady boundary layer which develops on a finite rotating disk in a counter-rotating fluid. It is found that the breakdown of the solution occurs at the axis at the same time, and thus the concept of a thin boundary layer in this more realistic problem is also destroyed in a finite time.

1. Introduction

Although the study of motions of a viscous fluid in which are immersed two parallel disks rotating coaxially in opposite senses goes back to Schultz-Grünow (1935), substantial difficulties and controversies remain at the present time. This situation is in marked contrast to that when the disks are rotating in the same sense or when one is at rest, about which a great deal has been discovered as was shown by the recent paper of Nguyen, Ribault & Florent (1975) and references quoted therein.

For two disks in counter-rotation at high Reynolds number (based on the distance between the disks) two contradictory solutions have been proposed. One of them, due to Stewartson (1953), suggests that the fluid motion is largely confined to boundary layers of von Kármán's form (1921) near each disk with the main body of fluid between the disks only slightly disturbed. This hypothesis has been verified in the coarse experiments described by Stewartson (1953).

† Permanent address: Department of Mathematics, University College London.

However, numerical studies (Lance & Rogers 1962; Pearson 1965) of the flow between two infinite disks rotating with angular velocities $\tilde{\Omega}$ and $\Omega_1 = \sigma\tilde{\Omega}$ ($\sigma < 0$) bear out this conclusion only when $\sigma = -1$. If $\sigma \neq -1$ the flow properties are more complicated and a substantial core flow seems to persist at large values of R. Even at $\sigma = -1$ Pearson found in the numerical work an apparent temporal instability at variance with the experiments and concluded that no stable symmetrical solution can exist. Later Tam (1969) suggested that the substantial stable core flows found by Pearson are inviscid but Matkowsky & Siegmann (1975) have demonstrated that his matching arguments fail if carried far enough. Also, certain rigorous properties of the governing equations have been established by McLeod & Parter (1974) which are consistent with Stewartson's experiments.

The other solution, possibly relevant when $R \gg 1$, assumes that the flow field when $\sigma < 0$ is basically similar to that when $\sigma > 0$, i.e. consists of a core of fluid rotating with angular velocity Ω and two boundary layers, one on each disk. This model, first suggested by Batchelor (1951), is intuitively attractive and, although it has not yet been observed, the properties of the resulting flow field are worth exploring. The model cannot be valid for all $\sigma < 0$ since we know that the boundary-layer equations have no solution if $\Omega_1 = -\Omega$ (McLeod 1970), and no numerical solutions of the equations have been found if

$$-6{\cdot}211 < \sigma < -0{\cdot}6879\dagger \tag{1.1}$$

(Evans 1969; Bodonyi 1975). Also, McLeod & Parter (1974) suggest that for the case $\Omega_1 = -\Omega$ the behaviour of the governing equations as $R \to \infty$ is not consistent with the solution suggested by Batchelor; although in the absence of a uniqueness proof a solution of Batchelor's type cannot be ruled out *a priori*.

In the present paper we attempt to advance our understanding of the flow field by discussing the transient problem, i.e. we examine the growth of the unsteady boundary layer from an initial, Rayleigh, form in one of the cases where no steady-state solution exists. We wish to examine whether the failure is due to an overly simple view of the steady-state solution or some other cause. The first possibility has already been met in related problems, namely the boundary layer induced by a potential vortex (Burggraf, Stewartson & Belcher 1971) or a generalized vortex (Belcher, Burggraf & Stewartson 1972) above a fixed disk. In these problems the non-existence of solutions of the steady-state similarity equations was resolved for a finite disk on the basis of a multi-structured boundary layer developing near the centre of the disk. It appears, however, that in the present instance the solution becomes singular at a finite value of Ωt^* in all components of the velocity. The phenomenon may be thought of as an explosion.

We first study problem I, in which two parallel infinite disks are initially rotating with angular velocity Ω about a common axis, the appropriate Reynolds

† Bodonyi (1975) gives an analytic argument which suggests that this number can be improved to $-0{\cdot}6968$. Recent detailed numerical studies by Prof. P. J. Zandbergen and Dr D. Dijkstra show that the solution is not unique below the point $\sigma = -6{\cdot}229$ and that a second branch arises which ranges back to positive values of σ.

number R being very large. At time $t^* = 0$ the angular velocity of one of these disks is suddenly reversed to become $-\Omega$. (The choice of an abrupt reversal is not crucial: so long as the reversal takes place within a few revolutions of the disk, the main conclusions would be unaltered.) Initially the fluid between the disks continues to rotate with angular velocity Ω apart from an unsteady and growing boundary layer set up near the disturbed disk. The growth of this boundary layer is studied numerically and it is found that it breaks down when $\Omega t^* = t_E \doteqdot 2{\cdot}36$ in a novel way: all the velocity components become infinite. Such a statement of course involves an element of inference because no numerical procedure can exhibit infinities: we mean that the numerical solution can be fitted to an asymptotic expansion containing such singularities in a moderately satisfactory way. We deduce that, within half a revolution of the occurrence of the abrupt reversal, the concept of a rotating core of fluid with a thin unsteady boundary layer has been destroyed and we can expect that thereafter the core flow must be modified in a serious way.

In light of previous studies (Burggraf *et al.* 1971) one possible explanation of this phenomenon is that, were the disks of finite radius, the unsteady similarity solution would hold only in the neighbourhood of the axis at best. Indeed the boundary layer moving inwards from the edge of the disk might take on a multi-structured form near the axis in which the radial velocity has a non-zero value at the axis, so that the unsteady similarity solution would be irrelevant. We investigate this possibility by studying problem II, in which three finite parallel disks are rotating coaxially with angular velocity Ω, the Reynolds number being large. The outer two disks each have radius b sufficiently large that the core of uniformly rotating fluid between them envelopes the central disk of radius $a\,(a < b)$. At time $t^* = 0$ the angular velocity of this central disk changes sign. Initially two Rayleigh-type boundary layers are set up on either side of the central disk. In them the radial velocity is negative and so the finite nature of the disk must affect the further development of the outer part of these boundary layers. The inner boundary of the affected part is at the edge when $t^* = 0$ and moves inboard at an exponentially decreasing rate, formally reaching the axis when $\Omega t^* = \infty$. It might be expected, therefore, that the unsteady similarity solution is valid near the axis so long as it exists and that the breakdown of the solution of the more general problem occurs at the axis at the same time t_E. The numerical study verifies this inference and thus the concept of a thin boundary layer in this more realistic problem is also destroyed in a finite time.

It is of interest to examine the behaviour of the unsteady boundary layer when $\sigma \neq -1$. Further work needs to be done but there are some unpublished studies by Bodonyi (1973). These concern problem I with $\sigma = -0{\cdot}10$, $-0{\cdot}25$ and $-0{\cdot}50$ and show that even when the steady-state solution exists it is not approached by the unsteady calculations as $\Omega t^* \to \infty$. Instead, for $\sigma = -0{\cdot}10$ the solution takes on the characteristics of a limit cycle, with, for example, the skin-friction vector describing a closed curve, points of which can be at a substantial distance from the corresponding steady-state value. For $\sigma = -0{\cdot}25$ and $-0{\cdot}50$ no limit-cycle solution was found. Instead the numerical computations failed to converge in a finite time, following a behaviour very similar to that for $\sigma = -1$. It may be that we can define three numbers σ_1, σ_2 and σ_3 such that

$$0 \geqslant \sigma_1 \geqslant \sigma_2 > \sigma_3 \tag{1.2}$$

with the properties that if $0 \geqslant \sigma \geqslant \sigma_1$ the steady state is the limit of the unsteady solution as $\Omega t^* \to \infty$, if $\sigma_1 > \sigma > \sigma_2$ the unsteady solution does not have a limit and grows indefinitely in width as Ωt^* increases, and if $\sigma_2 > \sigma > \sigma_3$ the unsteady solution breaks down at a finite time. These numbers do not necessarily coincide with those in (1.1) and indeed we cannot yet exclude the possibilities that $\sigma_1 = 0$ and $\sigma_3 = \infty$. The statements above may also provide the key to understanding why Stewartson (1953) was unable to obtain a core flow in his experiments with $\sigma < 0$.

These studies are also relevant in a quite different context. For a number of years there has been an increasing interest in unsteady separation, particularly with the possibility that a breakdown can occur at a finite time. An excellent review of the developments in the subject has recently been given by Sears & Telionis (1975). Examples are given in which singularities do occur but these are constructed by applying a similarity transformation reducing the number of independent variables from three to two so that the singularity must exist for all time. Williams & Johnson (1974) demonstrate a very good example of this type. In other studies a singularity has been claimed to begin at some finite time but since the unsteady solution is approaching a steady-state solution which is known to contain a singularity, such a claim must be treated with some caution until a systematic analytic procedure is available for describing the singularity. Sears & Telionis are optimistic that such a theory is close at hand. The only cases known to the authors in which the unsteady boundary layer exhibits grossly anomalous behaviour after a finite time, predicted numerically and verified analytically, are equivalent to the rear-stagnation study of Proudman & Johnson (1962). Here the boundary-layer thickness increased exponentially with time.

We claim, therefore, that the present problem is especially interesting as the first known example in which an unsteady boundary layer, initially well behaved, breaks down after a finite interval of time in a manner described in a mutually consistent way using numerical and analytic methods. Further, the breakdown takes on a quite different form from the steady breakdown at $\sigma = -0{\cdot}6968$ discussed by Bodonyi (1975) and from those discussed by Sears & Telionis (1975), being manifested by an infinite displacement thickness and infinite velocity components in all directions.

2. Problem I: the infinite disk

Consider an incompressible fluid with kinematic viscosity ν confined between the two parallel planes $z^* = 0$ and $z^* = d$. At first the fluid and the disks are assumed to be rotating rigidly with angular velocity Ω, then at time $t^* = 0$, the angular velocity of the plane $z^* = 0$ is instantaneously reversed. It is then reasonable to assume that if $R \gg 1$, where $R = \Omega d^2/\nu$ is the Reynolds number of the flow, the principal disturbance to the fluid is confined within a thin boundary layer near the plane $z^* = 0$ for a finite range of values of Ωt^*. Relative to cylindrical polar co-ordinates (r^*, θ, z^*) having as axis the common axis of rotation of the disks, the velocity components of the fluid can be written as

$$(\Omega r^* \,\partial F/\partial z, \Omega r^* G, \ -2(\nu\Omega)^{\frac{1}{2}} F), \tag{2.1}$$

where $z = z^*(\Omega/\nu)^{\frac{1}{2}}$, $t = \Omega t^*$, and F and G are functions of z and t only. Further, since $R \gg 1$ the governing equations may be reduced to boundary-layer form, i.e.

$$F_{zt} = F_{zzz} + 2FF_{zz} - F_z^2 + G^2 - 1, \tag{2.2a}$$

$$G_t = G_{zz} + 2FG_z - 2GF_z, \tag{2.2b}$$

where a suffix denotes a derivative. The equation of continuity is identically satisfied in virtue of (2.1). The appropriate boundary conditions are

$$F = F_z = 0, \quad G = 1 \quad \text{at} \quad t = 0 \quad \text{for all} \quad z, \tag{2.3a}$$

$$G \to 1, \quad F_z \to 0 \quad \text{as} \quad z \to \infty \quad \text{for all} \quad t, \tag{2.3b}$$

$$G = -1, \quad F = F_z = 0 \quad \text{at} \quad z = 0 \quad \text{for all} \quad t > 0. \tag{2.3c}$$

These equations were integrated numerically using a time-implicit finite-difference scheme wherein all derivatives are replaced by their corresponding centred-difference expressions. If q_j denotes a velocity component at the point z_j at the current time t and $\bar{q}_j$ its known value at the previous time $\bar{t} = t - \Delta t$, the difference equations are written for the intermediate time $t^* = \frac{1}{2}(\bar{t} + t)$ in the manner of Crank & Nicholson (1947) with $q_j^* = \frac{1}{2}(\bar{q}_j + q_j)$. The finite-difference analogues of (2.2) are expressed in matrix notation as

$$\mathbf{M}\mathbf{F}_z = \mathbf{R}, \quad \mathbf{M}\mathbf{G} = \mathbf{S}, \tag{2.4}$$

where $\mathbf{M}$ is a tridiagonal square matrix, $\mathbf{F}_z$ and $\mathbf{G}$ are column vectors representing the velocity components, and $\mathbf{R}$ and $\mathbf{S}$ column vectors whose elements contain both known and unknown functions of the flow properties. For a given time (2.4) were solved using Gaussian elimination for the simultaneous solution at all points within the domain with F being found during each cycle by integrating F_z. Since (2.2) are nonlinear it was necessary to use an iterative procedure, repeatedly solving (2.4) until the desired degree of convergence was obtained (say $|q' - q| < 10^{-5}$). Once convergence had been obtained at time t, the solution was advanced to the new time $t + \Delta t$ and the process repeated until the computations failed to converge.

The integration proceeded smoothly for $0 \leqslant t \leqslant 2{\cdot}0$ while for $t > 2$ the solution began to develop explosively with the boundary-layer thickness increasing to large values. The integration was terminated at $t = 2{\cdot}25$, when $F(\infty, t) \approx -221$ and the boundary-layer thickness had reached ≈ 60. We note that the boundary conditions (2.3b) at $z = \infty$ were replaced by the same conditions at $z = 60$. Further, the step lengths in t chosen were $\Delta t = 0{\cdot}01$ and $0{\cdot}005$ but the solution appeared to be insensitive to the change. On the other hand the step lengths Δz chosen for z had the values $0{\cdot}30$ and $0{\cdot}15$ and significant changes did appear as Δz varied. In presenting the final results h^2-extrapolation was used to estimate the solution in the double limit $\Delta z, \Delta t \to 0$.

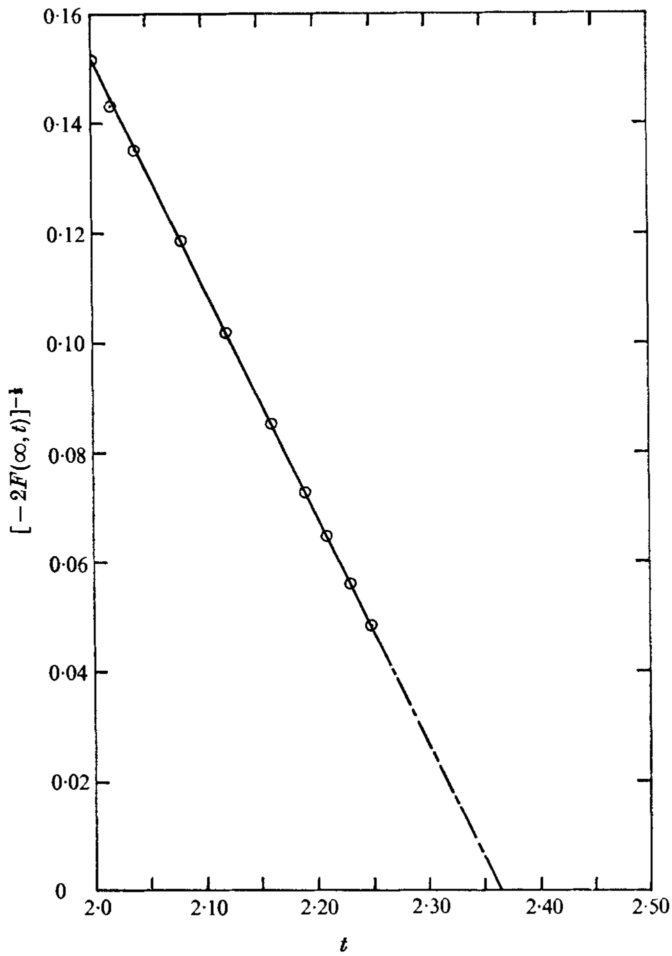

FIGURE 1. Variation of normal velocity $W_\infty(t) = -2F_\infty(t)$ at edge of boundary layer with t.

In figure 1 we present the variation of $[-2F(\infty,t)]^{-\frac{1}{2}}$ with t for $t \geqslant 2$ and in table 1 the variation of some of the characteristic properties of the solution near the final breakdown. In figure 2 we present curves of G and F_z for $t \geqslant 1{\cdot}0$.

A clue to the nature of the breakdown indicated by the numerical solution is provided by table 1 and figure 1, which suggest that $\{-2F(\infty,t)\}^{-\frac{1}{2}}$ varies linearly with t, vanishing at $t = t_E \approx 2{\cdot}365$. Thus near $t = t_E$

$$F(\infty,t) \approx -\pi/\alpha(t_E-t)^2, \quad \alpha \text{ a constant.} \tag{2.5}$$

By making use of this conjecture we shall initiate an asymptotic theory which describes the nature of the breakdown and provides additional authority for the numerical study. Since $G_z(0,t)$ and $F_{zz}(0,t)$ appear to remain finite while $-F(\infty,t)\to\infty$ as $t\to t_E$, we infer that, over the majority of the flow field, viscous forces are negligible in comparison with the inertial forces. On further taking

t	$-F(\infty, t)$	$\{-2F(\infty, t)\}^{-\frac{1}{2}}$	$-F_{zz}(0, t)$	$G_z(0, t)$
0	0	∞	0	∞
0·50	0·3152	1·2594	0·4450	1·527
1·00	1·138	0·6630	0·6373	0·9065
1·50	3·584	0·3735	0·7858	0·4381
2·00	21·77	0·1515	0·7883	−0·1509
2·19	95·88	0·0722	0·6684	−0·4145
2·21	122·2	0·0640	0·6491	−0·4419
2·23	160·5	0·0558	0·6284	−0·4689
2·25	220·9	0·0476	0·6062	−0·4956

TABLE 1

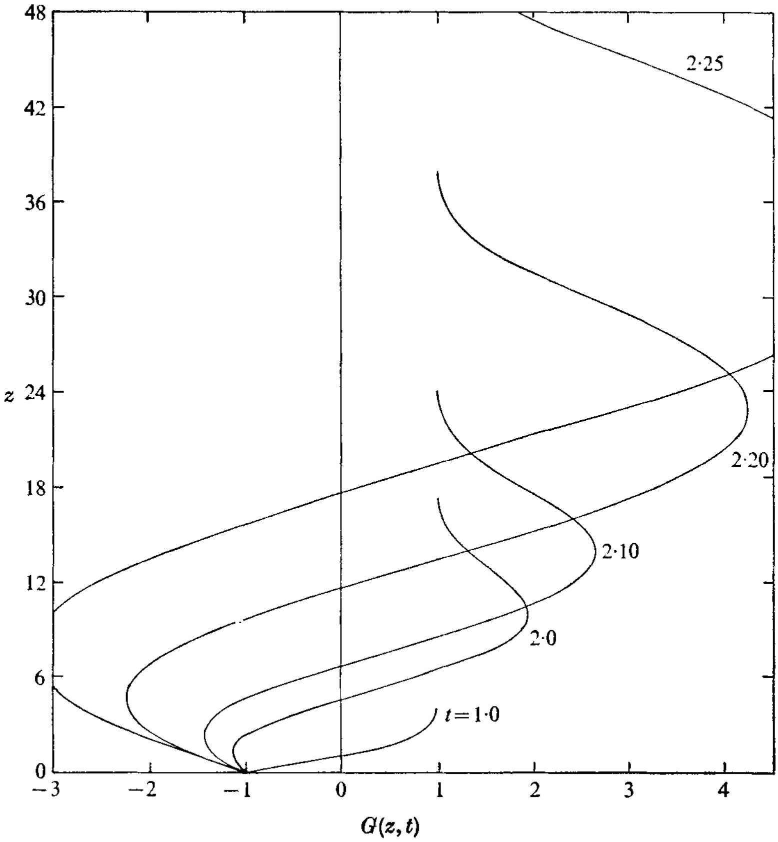

FIGURE 2(*a*). For legend see next page.

advantage of (2.5) we see that a consistent solution of the governing equations may be found by making the assumptions

$$\partial/\partial z \sim \tau, \quad G \sim \tau^{-1}, \quad F \sim \tau^{-2}, \quad \text{where } \tau = t_E - t.$$

The consequences of these assumptions are explored on a quantitative basis after rewriting the governing equations (2.2) in terms of the functions $H(\eta, \tau)$ and $K(\eta, \tau)$, where

$$\eta = \alpha z \tau, \quad \tau G = K(\eta, \tau), \quad \alpha \tau^2 F = H(\eta, \tau) - \tfrac{1}{2}\eta, \tag{2.6}$$

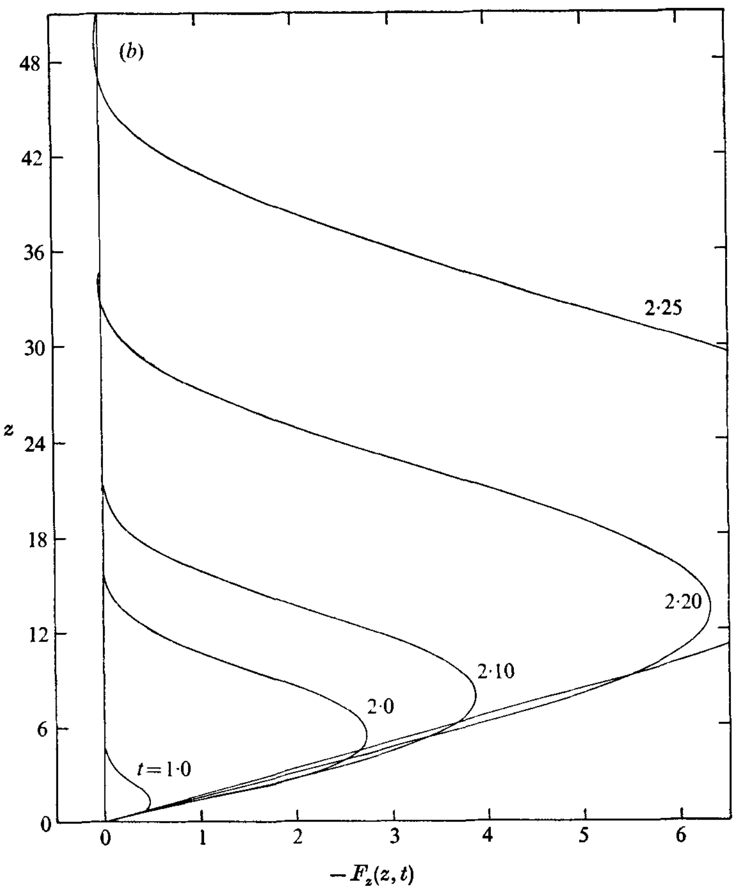

FIGURE 2. Variation of (a) $G(z,t)$ and (b) $F_z(z,t)$ with z for values of t near t_E.

α being a free constant at this point. Equations (2.2) then become

$$-\tau H_{\eta\tau} = 2HH_{\eta\eta} + K^2 - H_\eta^2 + \tfrac{1}{4} - \tau^2 + \alpha^2\tau^3 H_{\eta\eta\eta}, \tag{2.7a}$$

$$-\tau K_\tau = 2HK_\eta - 2H_\eta K + \alpha^2\tau^3 K_{\eta\eta}, \tag{2.7b}$$

with boundary conditions

$$H(0,\tau) = 0, \quad H_\eta(0,\tau) = \tfrac{1}{2}, \quad K(0,\tau) = -\tau, \tag{2.8a}$$

$$H_\eta(\infty,\tau) = \tfrac{1}{2}, \quad K(\infty,\tau) = \tau, \tag{2.8b}$$

and some initial condition at $t = t_E$ which we shall not need. In parentheses we note that other possible algebraic singularities of $F(\infty, t)$ as $\tau \to 0$ in which the exponent of $t_E - t$ differed from that in (2.5) were also examined; our studies indicated that it is unlikely that any exponent different from 2 could form the basis of an asymptotic expansion of the kind which we develop here.

Let us now assume that, for $\tau \ll 1$,

$$H(\eta,\tau) = H_0(\eta) + \tau H_1(\eta) + \dots, \tag{2.9a}$$

$$K(\eta,\tau) = K_0(\eta) + \tau K_1(\eta) + \dots. \tag{2.9b}$$

On substituting (2.9) into (2.7) and equating coefficients of τ^0, we obtain

$$H_0 K_0' - K_0 H_0' = 0, \tag{2.10a}$$

$$2H_0 H_0'' - H_0'^2 + K_0^2 + \tfrac{1}{4} = 0, \tag{2.10b}$$

the primes denoting differentiation with respect to η. Since α is a free constant we may, without significant loss of generality, deduce from (2.10*a*) that

$$H_0 + K_0 = 0. \tag{2.11}$$

The alternative solution is $H_0 = K_0$, which was excluded by a comparison with the numerical results. It is equivalent to replacing η by $-\eta$ and H_0 by $-H_0$. It follows from (2.11) and (2.10*b*) that

$$H_0'' + H_0 = \tfrac{1}{2}\beta, \tag{2.12}$$

where β is also a constant to be found. The boundary conditions for these functions at $\eta = 0$ are

$$K_0(0) = H_0(0) = 0, \quad H_0'(0) = \tfrac{1}{2}, \tag{2.13}$$

so

$$-K_0 = H_0 = \tfrac{1}{2}\sin\eta + \tfrac{1}{2}\beta(1-\cos\eta). \tag{2.14}$$

This solution satisfies the boundary conditions (2.13) but cannot satisfy those as $\eta \to \infty$. It must be joined, therefore, to another solution in which the viscous forces are significant. Indeed we can think of the viscous forces as acting in the neighbourhood of $z = 0$ when t is small, then as $t \to t_E$ being displaced away from this region by the inviscid solution (2.14) but nevertheless continuing to give the solution a characteristic diffusive property in the displaced region. Hence any match with the viscous region must require F_z and G to be finite and therefore occurs in the neighbourhood of $\eta = 2n\pi$, where n is an integer. An examination of the numerical results indicates that $n = 1$, but there is no intuitive reason why this should be so. Ockendon (1972) and Bodonyi (1975) found in related problems that analytically any integer choice of n could lead to a successful match.

Let us now consider the equations for H_1 and K_1 obtained by equating the coefficients of τ in the equations resulting from (2.7) when use is made of (2.9). On writing

$$K_1(\eta) = -H_1(\eta) + P_1(\eta), \tag{2.15}$$

we find that they reduce to

$$4H_0^2(P_1''' + P_1') + 4H_0 P_1'' + P_1'(1-2H_0') = 0, \tag{2.16}$$

$$2H_0 P_1' + (1-2H_0')P_1 = H_1. \tag{2.17}$$

Two of the complementary functions of (2.16) are simple, while the third has logarithmic singularities at $\eta = 0$ and 2π and can be excluded. Thus

$$P_1 = A + B(\eta + 2H_0), \tag{2.18}$$

where A and B are constants, which means that

$$H_1 = A(1-2H_0') + B[4H_0 + \eta(1-2H_0')], \tag{2.19a}$$

$$K_1 = 2AH_0' + 2B(\eta H_0' - H_0). \tag{2.19b}$$

The boundary conditions on H_1 and K_1 at $\eta = 0$ are

$$K_1(0) = -1, \quad H_1(0) = H_1'(0) = 0 \tag{2.20}$$

from (2.8a), so that

$$A = -1, \quad B = -\tfrac{1}{2}\beta. \tag{2.21}$$

Let us now consider the behaviour of the inner solution near $\eta = 2\pi$. We set

$$\hat{z} = z - 2\pi/\alpha\tau, \tag{2.22}$$

express those terms of the series (2.9) that have been calculated as functions of $\hat{z}$ and τ, and then expand once more in powers of τ. We obtain

$$G = -1-\beta\pi-\tfrac{1}{2}\alpha\hat{z}-\alpha\beta\tau\{(1+\beta\pi)\hat{z}+\tfrac{1}{4}\alpha\hat{z}^2\}+O(\tau), \tag{2.23a}$$

$$F = -\pi/\alpha\tau^2+\pi\beta^2\hat{z}+\tfrac{1}{4}\alpha\beta\hat{z}^2+O(1). \tag{2.23b}$$

It is clear that (2.23) is incompatible with the boundary conditions (2.3b) as $z\rightarrow\infty$, so there must be another region near $\eta = 2\pi$ in which viscous forces are significant. Let us adopt $\hat{t} = t$ and $\hat{z}$ as the new independent variables and write

$$F+\pi/\alpha\tau^2 = \hat{F}(\hat{z},\hat{t}), \quad \hat{G}(\hat{z},\hat{t}). \tag{2.24}$$

Then the equations for $\hat{F}$ and $\hat{G}$ are identical with (2.2) on supplying the appropriate carets and the boundary conditions become, when $\tau = 0$,

$$\hat{G}\rightarrow 1, \quad \hat{F}_{\hat{z}}\rightarrow 0 \quad \text{as} \quad \hat{z}\rightarrow+\infty, \tag{2.25a}$$

$$\hat{G}+\tfrac{1}{2}\alpha\hat{z}\rightarrow -1-\beta\pi, \quad \hat{F}_{\hat{z}}-\tfrac{1}{2}\alpha\beta\hat{z}\rightarrow\pi\beta^2 \quad \text{as} \quad \hat{z}\rightarrow-\infty. \tag{2.25b}$$

Conditions (2.25) are, however, insufficient to determine the leading terms in the asymptotic expansions of $\hat{F}$ and $\hat{G}$ in powers of τ when $\hat{z}$ is finite; indeed any smooth functions of $\hat{z}$ satisfying (2.25) may be regarded as candidates for these terms. The correct forms depend in some way on the initial conditions when $\hat{t} = 0$ and on the boundary conditions at the disk, where $z = 0$. For further terms we need more information from the inner solution valid when η is finite and this presents some difficulty, which we shall discuss below.

The validity of the structure proposed above can in part be tested by comparison with the numerical solution. First of all we see from (2.24) that $\hat{F}$ is likely to be a finite function of $\hat{t}$ as $\tau\rightarrow 0$, so that $\alpha(t_E-t)^2\, F(\infty,t)\rightarrow -\pi$ as $t\rightarrow t_E$. The graph of $W_\infty(t) = -2F(\infty,t)$ displayed in figure 1 is consistent with this statement. Further, the graphs of F_z and G in figure 2 show an explosive character near $t = t_E$ ($\simeq 2{\cdot}365$) but when scaled in terms of $[W_\infty(t)]^{\frac{1}{2}}$ remain finite and show fairly strong signs of approaching limits as $t\rightarrow t_E$ as shown in figures 3 (a) and (b). Also, the graphs of these limit curves appear to be quite close to the forms predicted by (2.14) on choosing the values of α and β appropriately. Again according to the asymptotic analysis

$$G_z(0,\tau) = -\tfrac{1}{2}\alpha-\alpha\beta\tau+\ldots, \tag{2.26a}$$

$$F_{zz}(0,\tau) = \tfrac{1}{2}\alpha\beta-\alpha\tau+\ldots; \tag{2.26b}$$

from table 1 and additional data not reproduced here it is clear that the numerical behaviour of these functions is consistent with their being smooth functions of

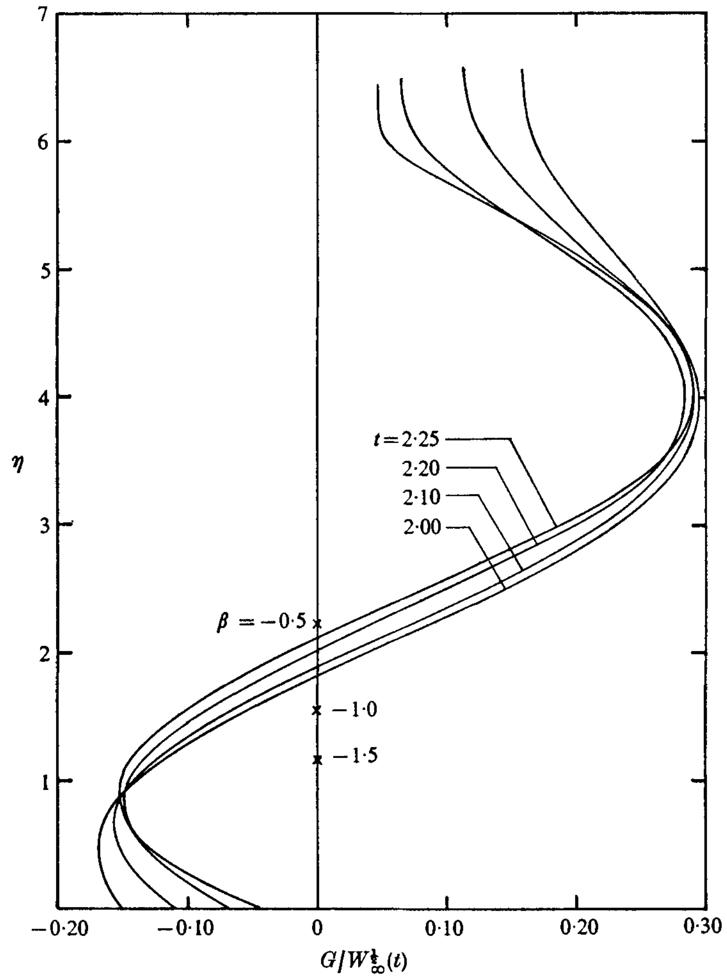

FIGURE 3 (*a*). For legend see next page.

τ near $\tau = 0$. Thus on general grounds we have substantial confidence that the solution does develop a singularity in the neighbourhood of $t = 2{\cdot}365$ and the limit structure is then as proposed by the analysis of this section.

However a cautionary note must now be struck. From each of the comparisons mentioned above the values of α and/or β can be inferred; however they are not quite consistent with each other. It seems that $\alpha \simeq 1{\cdot}1$ and $\beta \simeq -1$ are the best choices that can be made, but by using (2.5), (2.26), the values of $\max G(z,t)$ and $\max F_z(z,t)$, the values of z at which $G = 0$ and $F_z = 0$, and other devices to compute α and β we find discrepancies of up to 30 % in these estimates. It may be that the difficulties of carrying through the numerical integration for $t > 2{\cdot}2$ preclude the possibility of obtaining a fully consistent comparison, particularly for the fine details of the solution. Nevertheless we cannot completely exclude the possibility that the asymptotic expansion proposed is deceptively attractive and that at some later stage leads to a contradiction which cannot be overcome

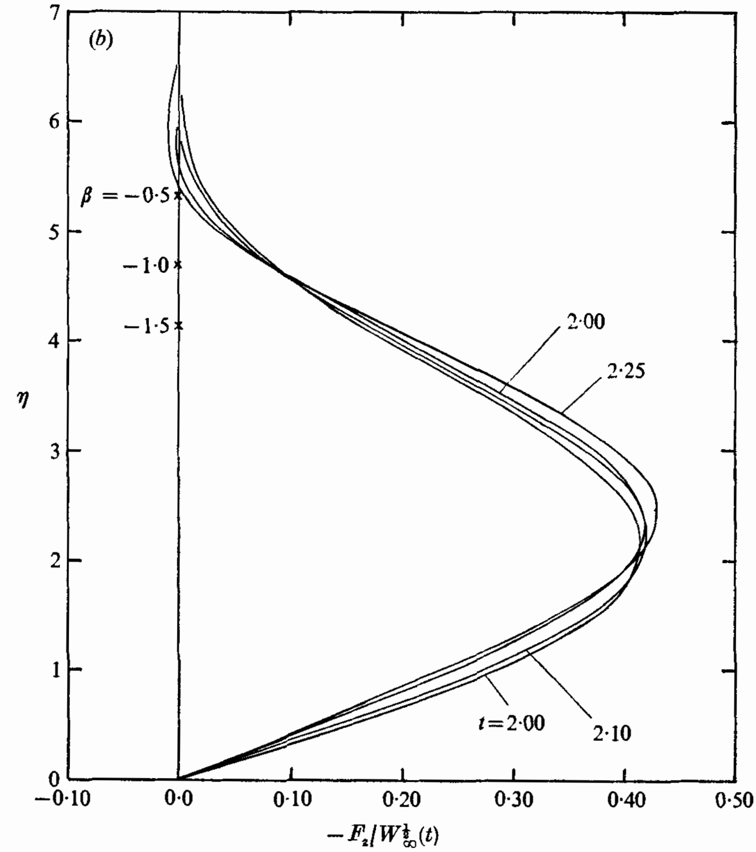

FIGURE 3. Variation of (*a*) $G/W_\infty^{\frac{1}{2}}(t)$ and (*b*) $F_z/W_\infty^{\frac{1}{2}}(t)$ with $\eta = \alpha z(t_E - t)$ for values of t near t_E. The crosses on the η axis indicate the zeros of (*a*) G_0 or (*b*) $H_0 - \frac{1}{2}\eta$ for $\beta = -0{\cdot}5$, $-1{\cdot}0$, and $-1{\cdot}5$.

and destroys its whole basis. In this connexion we note that determination of the next term, if it is assumed to be $O(\tau^2)$, in the expansion (2.9) involves the solution of the equation

$$H_0^2(P_2'''' + P_2') + 2H_0 P_2'' + (1 - H_0) P_2' = F_2(\eta), \tag{2.27}$$

where $F_2(\eta)$ is a function of η defined by the terms of (2.9) already found and P_2 is defined by an equation analogous to (2.15). The solution of this equation can in principle be non-analytic when $H_0 = 0$, i.e. $\eta = 0$, η_0 or 2π, where $\cot(\frac{1}{2}\eta_0) = -\beta$. A similar situation arises with the equation for P_1 but in that case the singularities may be avoided. Some numerical studies of P_2 have been made and it appears that the difficulties at $\eta = 0$ and η_0 can be avoided, but that P_2 is singular at $\eta = 2\pi$ for all β. Further, if additional terms of the series in (2.9) are calculated parallel difficulties to that with P_2 are likely to occur. It may be that the expansion forms adopted so far are not general enough to provide a complete asymptotic expansion for this flow field. Some support for this view is provided by the fact that the singularity in the solution for P_2 can be confined to $\eta = 2\pi$, at the end of its range of validity, and might, therefore, be removed or absorbed by some combination of an intermediate layer, where $\hat{z}$ is large and negative, and an expansion of the solution for $\hat{F}$ and $\hat{G}$ in non-integral powers of τ. For such an expansion the properties of the leading terms are important and we are able to obtain only numerical approximations to these at present.

In our opinion, balancing up these arguments, there is a reasonable case for believing that the solution of (2.2) does break down at a finite value of t as the numerical integration indicates. Further the inner structure of the solution, i.e. for finite values of z, takes on the form (2.9), (2.14) in the limit as $\tau \to 0$ and is essentially inviscid in character. The outer solution, in which viscous forces are significant, is then displaced towards $z = \infty$. We now consider problem II, which sets the present problem in a physically more realistic context.

3. Problem II: the finite disk

As explained in the introduction we now attempt to place the study of § 2 in a more physically satisfying context by supposing that a disk of radius a is placed in the plane $z^* = 0$ and two disks each of radius b ($\gg a$) are placed on either side in parallel planes. The disks are surrounded by an infinite volume of incompressible viscous fluid and initially are all rotating about a common axis through their centres with angular velocity Ω, so that a core of rigidly rotating fluid envelops the central disk. The angular velocity of this disk is now impulsively reversed in sign and we examine the unsteady boundary layer which is thereby induced on its upper side, $z^* > 0$. We write $r^* = ar$ and $t = \Omega t^*$, take the velocity components of the fluid to be

$$\{a\Omega u(r,z,t), \quad a\Omega v(r,z,t), \quad (\nu\Omega)^{\frac{1}{2}} w(r,z,t)\}, \tag{3.1}$$

and now let $R = \Omega a^2/\nu$ be large. The governing equations of this boundary layer reduce to

$$\frac{\partial u}{\partial t} + u\frac{\partial u}{\partial r} + w\frac{\partial u}{\partial z} - \frac{v^2}{r} = -r + \frac{\partial^2 u}{\partial z^2}, \tag{3.2a}$$

$$\frac{\partial v}{\partial t} + u\frac{\partial v}{\partial r} + w\frac{\partial v}{\partial z} + \frac{uv}{r} = \frac{\partial^2 v}{\partial z^2}, \tag{3.2b}$$

$$\frac{1}{r}\frac{\partial}{\partial r}(ru) + \frac{\partial w}{\partial z} = 0, \tag{3.2c}$$

with boundary conditions

$$u = 0, \quad v = -r, \quad w = 0 \quad \text{at} \quad z = 0, \quad r < 1 \quad \text{for} \quad t > 0, \tag{3.3a}$$

$$u = 0, \quad v = 1 \quad \text{at} \quad z > 0, \quad r = 1 \quad \text{for} \quad t > 0, \tag{3.3b}$$

$$u \to 0, \quad v \to r \quad \text{as} \quad z \to \infty \quad \text{for} \quad r \geqslant 0, \quad t > 0, \tag{3.3c}$$

$$u = 0, \quad v = r \quad \text{at} \quad t = 0 \quad \text{for all} \quad r > 0, \quad z > 0. \tag{3.3d}$$

Of these conditions (3.3a) describes the motion of the central disk $z = 0$ while the others express the fact that the central core of rotating fluid is presumed to be unaffected to first order by the growing boundary layers near $z = 0$.

The initial solution, when $0 < t \ll 1$ and $r < 1$, is the same as for the infinite disk discussed in the previous section and the radial velocity $a\Omega u$ is negative. Hence at a given value $\tilde{r} < 1$ of r, u/r and v/r are functions of z and t only for $t < T(r)$, where

$$(dT/dr)^{-1} = r \max\{-F_z(z,t)\} \quad \text{at} \quad r = \tilde{r}, \quad t = T, \tag{3.4}$$

where F is defined in § 2 and the maximum is taken over all $z > 0$. At subsequent times u/r and v/r are functions of r as well as of z and t. The general argument underlying (3.4) has been discussed by Stewartson (1960) and may be stated in physical terms as follows. The disturbance to the solution of § 2 caused by the finite size of the disk originates at the outer edge at $t = 0+$ then travels inwards at a speed equal to the negative radial component of the fluid velocity and simultaneously diffuses instantaneously to all values of z. Hence the disturbance front at any time is perpendicular to the disk. Further the global speed of propagation of this edge disturbance is equal to $-\max(a\Omega u)$ taken over all z at the given time and at the instantaneous position of the disturbance front.

Once u/r and v/r become functions of r as well as z and t a number of special features arise. In particular there is a singularity at $r = 1$ which needs special care. In order to examine these features and to facilitate the numerical computations to be discussed below we define new variables

$$\left.\begin{array}{ll} y = z/(1-r)^{\frac{1}{4}}, & u = r(1-r)^{\frac{1}{2}}U(r,y,t), \\ v = rV(r,y,t), & w = (1-r)^{-\frac{1}{4}}W(r,y,t). \end{array}\right\} \tag{3.5}$$

Thus the boundary-layer equations become

$$(1-r)^{\frac{1}{2}}\frac{\partial U}{\partial t} = \frac{\partial^2 U}{\partial y^2} - (W + \tfrac{1}{4}ryU)\frac{\partial U}{\partial y} - r(1-r)\,U\frac{\partial U}{\partial r} - 1 + V^2 + (\tfrac{5}{2}r - 1)\,U^2, \tag{3.6a}$$

$$(1-r)^{\frac{1}{2}}\frac{\partial V}{\partial t} = \frac{\partial^2 V}{\partial y^2} - (W + \tfrac{1}{4}ryU)\frac{\partial V}{\partial y} - r(1-r)\,U\frac{\partial V}{\partial r} - 2(1-r)\,UV, \tag{3.6b}$$

$$\frac{\partial W}{\partial y} + \tfrac{1}{4}ry\frac{\partial U}{\partial y} + r(1-r)\frac{\partial U}{\partial r} + (2 - \tfrac{5}{2}r)\,U = 0, \tag{3.6c}$$

with boundary conditions

$$U = 0, \quad V = -1, \quad W = 0 \quad \text{at} \quad y = 0, \quad r < 1 \quad \text{for} \quad t > 0, \tag{3.7a}$$

$$U = 0, \quad V = 1 \quad \text{at} \quad y > 0, \quad r = 1 \quad \text{for} \quad t > 0, \tag{3.7b}$$

$$U \to 0, \quad V \to 1 \quad \text{as} \quad y \to \infty \quad \text{for} \quad r \geqslant 0, \quad t > 0, \tag{3.7c}$$

$$U = 0, \quad V = 1 \quad \text{at} \quad t = 0 \quad \text{for all} \quad r > 0, \quad y > 0. \tag{3.7d}$$

In terms of these variables the governing equations have smooth solutions when y is finite, $0 < r < 1$ and t is finite.

The solution at $r = 1$ immediately takes on the steady-state similarity form and the appropriate equations obtained by setting $r = 1$ in (3.6) have been solved numerically by Bodonyi & Stewartson (1975). They discovered that there are in fact three possible solutions in one of which $V \equiv -1$ and in another of which $V + 1$ remains very small until y is large. Both of these solutions were

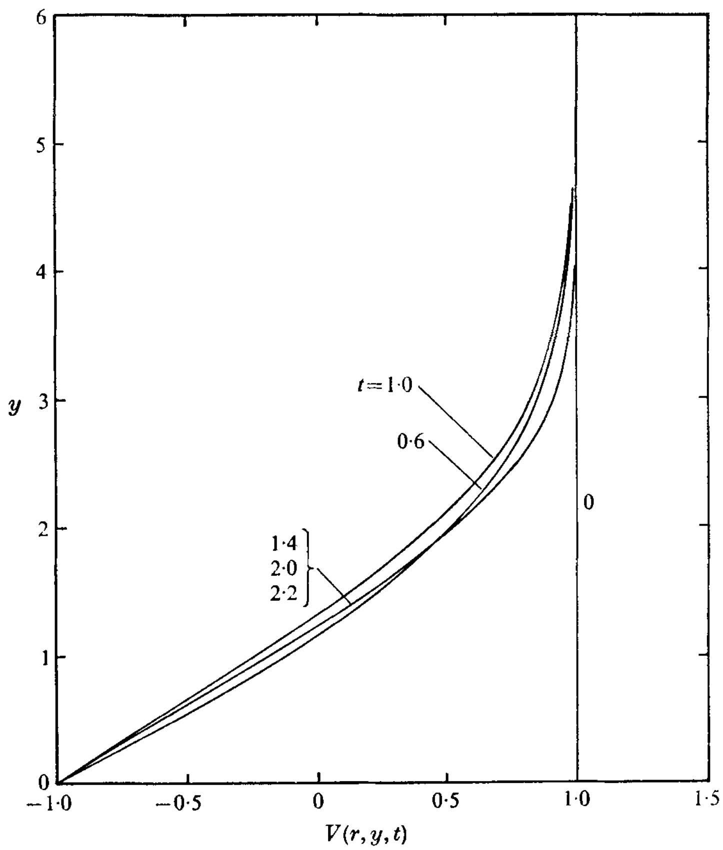

FIGURE 4 (*a*). For legend see next page.

rejected and the third, in which V becomes close to its mainstream value of $+1$ at moderate values of y, was chosen as the initial profile at $r = 1$. The resulting numerical solution behaved smoothly when $0 < 1-r \ll 1$.

Also, Belcher *et al.* (1972) have shown that if, as here, the circulation of the outer flow is an increasing function of the radius then the radial and tangential velocity profiles of the steady boundary layer both oscillate about their inviscid values for any $r < 1$ with amplitudes that diminish exponentially as the outer edge of the boundary layer is approached. Hence in the present problem we can expect regions of reversed flow which require some care in the numerical computations.

The numerical method chosen to integrate (3.2) is the same as that developed by Belcher (1970) and used (1972) to elucidate the structure of the generalized-vortex boundary layer. If q_{ij} denotes a velocity component at the node point (r_i, y_j) for the current time t and $\bar{q}_{ij}$ its known value at the previous time $\bar{t} = t-\Delta t$, the difference equations are written for the intermediate time $\bar{t}+\frac{1}{2}\Delta t$ in the manner of Crank & Nicholson (1947), with velocity components being replaced by their mean values $\frac{1}{2}(\bar{q}_{ij}+q_{ij})$, derivatives with respect to y by centred differences, and those with respect to r by downwind differences. The radial

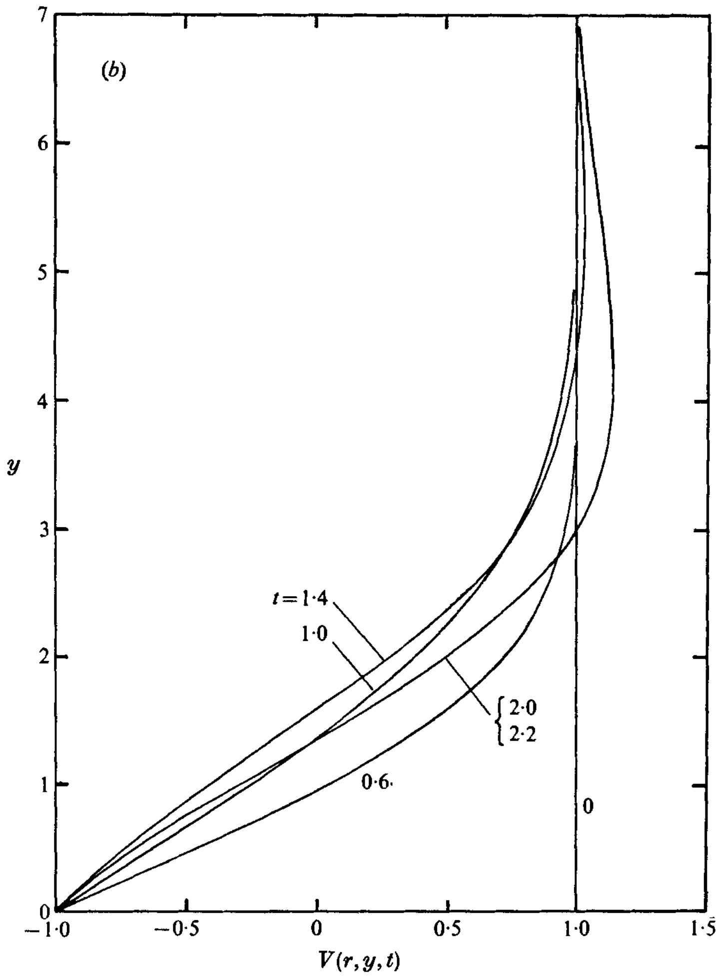

FIGURE 4. Variation of $V(r, y, t)$ with $y = z/(1-r)^{\frac{1}{2}}$ at (a) $r = 0{\cdot}80$ and (b) $r = 0{\cdot}60$ for selected values of t.

derivatives were, however, evaluated at the old time $\bar{t}$, thereby making the scheme partially explicit. Also, in Belcher's problems it was not possible to extend the solution as far as $r = 0$ in general, but no such difficulty arises here and a solution for all r is found for $t \leqslant 2{\cdot}28$. For the calculations the step lengths chosen were $\Delta r = 0{\cdot}05$, $\Delta y = 0{\cdot}30$ and $\Delta t = 0{\cdot}02$ and $0{\cdot}04$, and the outer edge of the boundary layer $y \to \infty$ was approximated by $y = 60$. These choices enabled us to achieve a reasonable balance between accuracy and computation time. Only the results of the computations will be presented here; further details on the numerical method are given by Bodonyi (1973).

As already mentioned, at $r = 1$ the solution immediately takes on its steady-state behaviour. For $r < 1$ the solution is dependent on t as well as on r and y. Near the outer part of the disk a steady state has virtually been reached by $t = 2$ as shown by the tangential velocity profiles at $r = 0{\cdot}8$ and $0{\cdot}6$ in figures

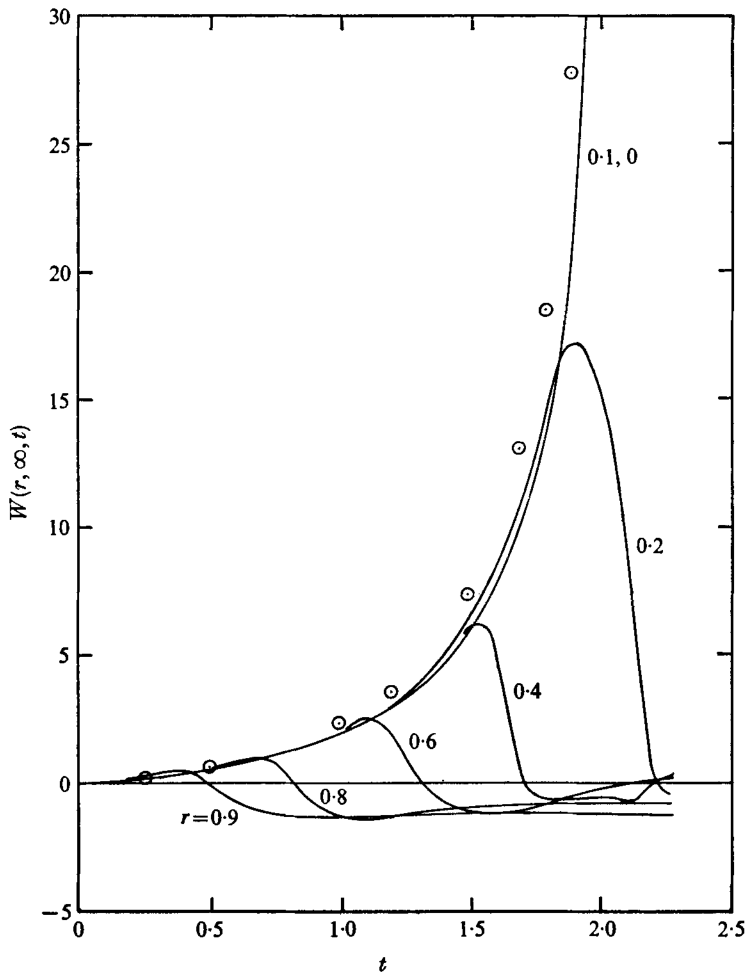

FIGURE 5. Variation of $W(r, \infty, t)$ with t for selected values of r. ⊙, results from the infinite-disk solution.

4(*a*) and (*b*) respectively. Over the inner part, however, there is no such clear indication and indeed the velocity components are rapidly increasing functions of t when $r = 0{\cdot}20$ and $t > 2$. We illustrate the situation by displaying the variation of $W(r, \infty, t)$, the normal velocity at the upper edge of the boundary layer, as a function of t for various values of r in figure 5. In figures 6(*a*) and (*b*) respectively, we display $V_y(r, 0, t)$ and $U_y(r, 0, t)$, the two components of the skin friction, as a function of r for various values of t. From figure 5 we see that there appears to be a massive eruption of the boundary layer at $t \approx 2{\cdot}3$ and near $r = 0$ whose character is very similar to that described in § 2. Elsewhere the boundary layer begins by acting as a centripetal fan but soon changes over to a centrifugal form, starting at the outer edge and moving inboard. Presumably the changeover occurs because of the necessity to feed the eruption at the centre. Figure 5 also gives further evidence that the steady-state behaviour near the

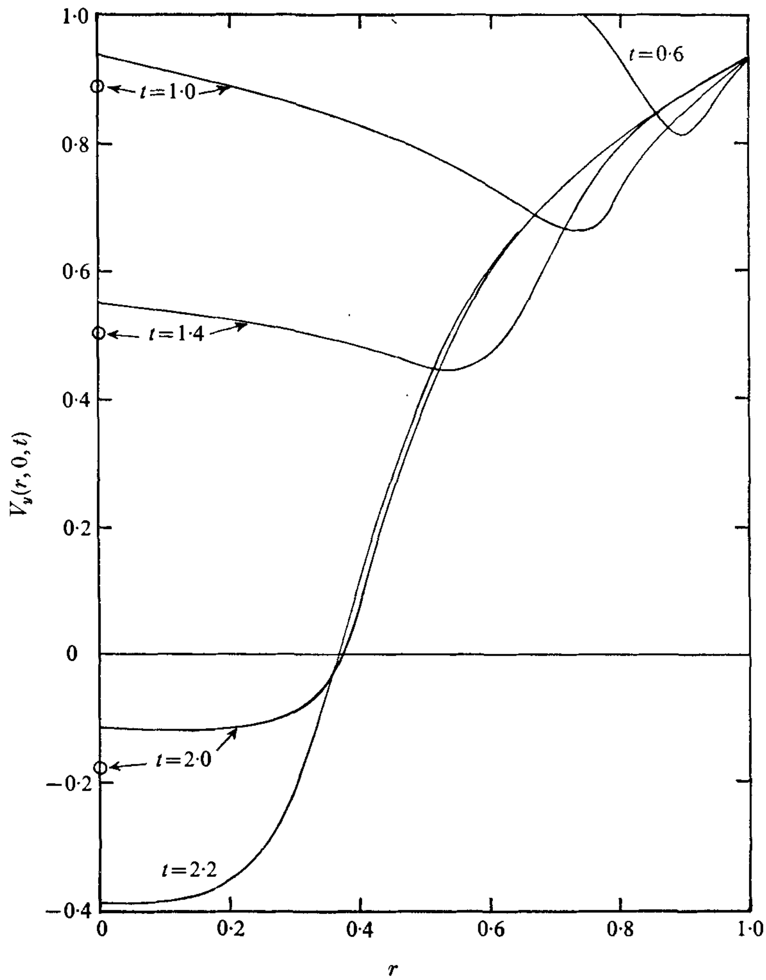

FIGURE 6 (*a*). For legend see facing page.

edge of the disk is reached rather quickly. In figure 6 (*a*) we see that the torque remains finite for all (r, t) and can readily imagine that there is a limiting curve of V_y for all r at $t = t_E$. Although the radial skin friction in figure 6 (*b*) is also finite it is not so easy to envisage a limiting form for it as $t \to t_E$.

The differences between the results of the present study at $r = 0$ and those for the finite disk discussed in the previous section can be seen in figures 5 and 6, wherein the corresponding infinite-disk solutions are given as circled points. The discrepancies between the results for the larger values of t are attributed to the differences in the step sizes Δr, Δz and Δt used in the numerical computations. A further comparison of the results near $r = 0$ indicates that the finite nature of the disk has little effect on the singularity, the two solutions being very nearly the same. As mentioned in the introduction this can be understood as follows. The disturbance front, behind which the solution depends on the finiteness of the disk, moves inboard with a velocity $r\gamma(r)$ which is the maximum inward radial velocity

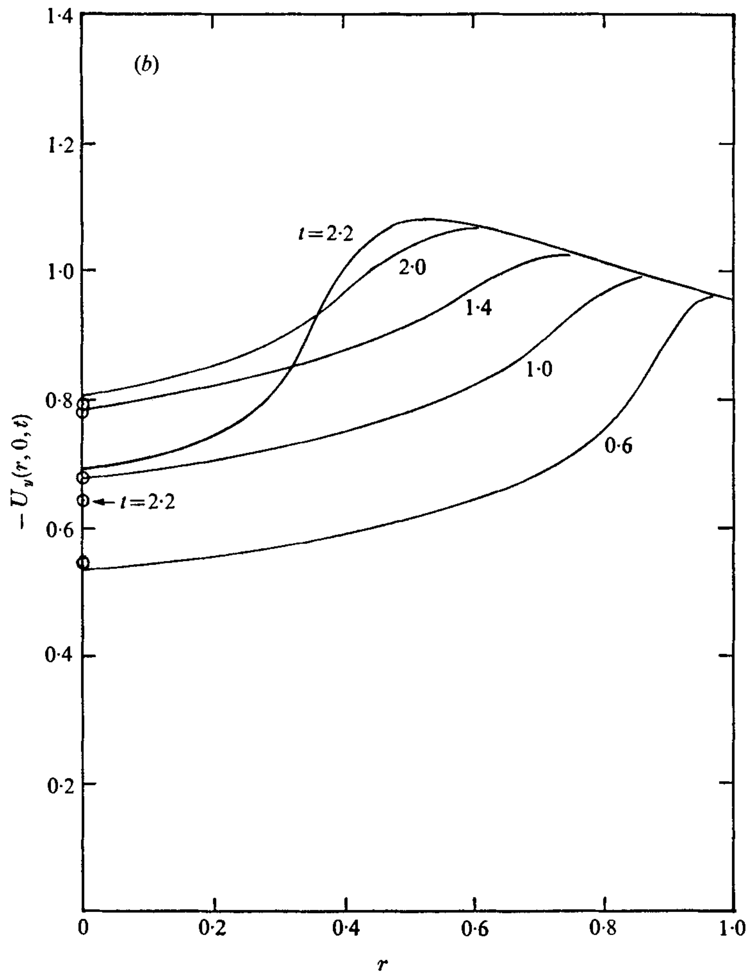

FIGURE 6. Variation of (a) tangential wall shear $V_y(r, 0, t)$ and (b) radial wall shear $U_y(r, 0, t)$ with r for selected values of t. ⊙, results from the infinite-disk solution.

at the front. Hence it cannot reach the origin in a finite time unless γ becomes infinite and so the singularity in the infinite-disk problem also occurs in the more realistic finite-disk problem at the axis of rotation.

The authors are grateful to Prof. O. R. Burggraf, who guided the graduate work of one of us (R.J.B.), for many helpful discussions and comments, particularly on the numerical procedure. They are also indebted to the computer centres of The Ohio State University and Virginia Polytechnic Institute and State University for making computer time available during the course of this study.

REFERENCES

BATCHELOR, G. K. 1951 Note on a class of solutions of the Navier–Stokes equations representing steady rotationally-symmetric flow. *Quart. J. Mech. Appl. Math.* **4**, 29.

BELCHER, R. J., BURGGRAF, O. R. & STEWARTSON, K. 1972 On generalized-vortex boundary layers. *J. Fluid Mech.* **52**, 753.

BODONYI, R. J. 1973 The laminar boundary layer on a finite rotating disc. Ph.D. dissertation, The Ohio State University.

BODONYI, R. J. 1975 On rotationally symmetric flow above an infinite rotating disk. *J. Fluid Mech.* **67**, 657.

BODONYI, R. J. & STEWARTSON, K. 1975 Boundary-layer similarity near the edge of a rotating disk. *J. Appl. Mech.* **42**, 584.

BURGGRAF, O. R., STEWARTSON, K. & BELCHER, R. J. 1971 The boundary layer induced by a potential vortex. *Phys. Fluids*, **14**, 1821.

CRANK, J. & NICHOLSON, P. 1947 A practical method for numerical evaluation of solutions of partial differential equations of the heat-conduction type. *Proc. Camb. Phil. Soc.* **43**, 50.

EVANS, D. J. 1969 The rotationally symmetric flow of a viscous fluid in the presence of an infinite rotating disc with uniform suction. *Quart. J. Mech. Appl. Math.* **22**, 467.

KÁRMÁN, T. VON 1921 Über laminare und turbulente Reibung. *Z. angew. Math.* **1**, 233.

LANCE, G. N. & ROGERS, M. H. 1962 The axially symmetric flow of a viscous fluid between two infinite rotating disks. *Proc. Roy. Soc.* A **266**, 109.

MCLEOD, J. B. 1970 A note on rotationally symmetric flow above an infinite rotating disc. *Mathematika*, **17**, 243.

MCLEOD, J. B. & PARTER, S. V. 1974 On the flow between two counter-rotating infinite plane disks. *Arch. Rat. Mech. Anal.* **54**, 301.

MATKOWSKY, B. J. & SIEGMANN, W. L. 1975 The flow between counter-rotating disks at high Reynolds number. *SIAM J. Appl. Math.* **30**, 720.

NGUYEN, N. D., RIBAULT, J. P. & FLORENT, P. 1975 Multiple solutions for flow between coaxial disks. *J. Fluid Mech.* **68**, 369.

OCKENDON, H. 1972 An asymptotic solution for the steady flow above an infinite rotating disc with suction. *Quart. J. Mech. Appl. Mech.* **25**, 291.

PEARSON, C. E. 1965 Numerical solutions for the time-dependent viscous flow between two rotating coaxial disks. *J. Fluid Mech.* **21**, 623.

PROUDMAN, I. & JOHNSON, K. 1962 Boundary-layer growth near a rear stagnation point. *J. Fluid Mech.* **12**, 161.

SCHULTZ-GRÜNOW, F. 1935 Der Reibungswiderstand rotierender Scheiben in Gehäusen. *Z. angew. Math. Mech.* **15**, 191.

SEARS, W. R. & TELIONIS, D. P. 1975 Boundary-layer separation in unsteady flow. *SIAM J. Appl. Math.* **28**, 215.

STEWARTSON, K. 1953 On the flow between two rotating coaxial disks. *Proc. Camb. Phil. Soc.* **49**, 333.

STEWARTSON, K. 1960 The theory of unsteady laminar boundary layers. *Adv. in Appl. Mech.* **6**, 1.

TAM, K. K. 1969 A note on the asymptotic solution of the flow between two oppositely rotating infinite plane disks. *SIAM J. Appl. Math.* **17**, 1305.

WILLIAMS, J. C. & JOHNSON, W. D. 1974 Semisimilar solutions to unsteady boundary-layer flows including separation. *A.I.A.A. J.* **12**, 1388.